

MICROSTRUCTURAL ANALYSIS OF FERRITIC-MARTENSITIC STEELS IRRADIATED AT LOW TEMPERATURE IN HFIR - N. Hashimoto (Oak Ridge National Laboratory), E. Wakai (Japan Atomic Energy Research Institute), J. P. Robertson (ORNL), and A. F. Rowcliffe (ORNL)

OBJECTIVE

The purpose of this work is to investigate the microstructural evolution of ferritic/martensitic steel irradiated at low temperatures to damage levels of about 3 dpa in order to relate the microstructure to the mechanical properties, in particular the fracture toughness and the yield strength.

SUMMARY

Disk specimens of ferritic-martensitic steel, HT9 and F82H, irradiated to damage levels of ~3 dpa at irradiation temperatures of either ~90°C or ~250°C have been investigated by using transmission electron microscopy. Before irradiation, tempered HT9 contained only $M_{23}C_6$ carbide. Irradiation at 90°C and 250°C induced a dislocation loop density of $1 \times 10^{22} \text{ m}^{-3}$ and $8 \times 10^{21} \text{ m}^{-3}$, respectively. In the HT9 irradiated at 250°C, a radiation-induced phase, tentatively identified as α' , was observed with a number density of less than $1 \times 10^{20} \text{ m}^{-3}$. On the other hand, the tempered F82H contained $M_{23}C_6$ and a few MC carbides; irradiation at 250°C to 3 dpa caused minor changes in these precipitates and induced a dislocation loop density of $2 \times 10^{22} \text{ m}^{-3}$. Difference in the radiation-induced phase and the loop microstructure may be related to differences in the post-yield deformation behavior of the two steels.

PROGRESS AND STATUS

1. Introduction

Ferritic/martensitic steels are attractive candidate structural first wall materials for fusion reactors [1]. Neutron irradiation at low temperature can cause an increase in the yield stress and a decrease in the uniform elongation, as determined by tensile test. Additionally the ductile-brittle transition temperature (DBTT) may increase and the upper shelf energy may decrease, as determined by a Charpy impact test. It was previously reported [2] that irradiation of HT9 to ~3 dpa in HFIR at 250 °C resulted in an increase in yield stress of about 450 MPa accompanied by a reduction in uniform elongation from 12% to 6% when tested at the irradiation temperature. Although the F82H underwent somewhat less hardening ($\Delta YS=350 \text{ MPa}$) at 250°C, the uniform elongation was reduced to less than 0.5%. In spite of the loss of strain hardening capacity observed for the F82H, the fracture toughness values of both alloys were similar at 250°C. In addition, the F82H maintained good toughness at room temperature; on the other hand, the HT9 exhibited lower-shelf brittle behavior at room temperature.

The objective of the this study is to investigate microstructure of ferritic/martensitic steels, HT9 and F82H, irradiated at low temperatures and to damage levels of about 3 dpa in order to relate the microstructure to the mechanical properties, in particular the fracture toughness and the yield strength.

2. Experimental Procedure

HT9 and F82H were included in this experiment; the compositions are given in Table 1. Standard 3-mm diameter transmission electron microscopy (TEM) disks were punched from 0.25-mm thick sheet stock, and then these disk were normalized and tempered as indicated in Table 2.

Table 1. Chemical compositions of F82H and HT9 (wt%). (Balance Fe)

Steel	Cr	Ni	Mo	Mn	Si	C	N	V	W	Ta	P	S
HT9	12.1	0.51	1.04	0.57	0.17	0.20	0.027	0.28	0.45	-	.016	.003
F82H	7.65	0.05	-	0.49	0.09	0.093	0.002	0.18	1.98	0.038	.001	.001

Table 2. Normalizing and tempering conditions for F82H and HT9.

Steel	Normalizing	Tempering
HT9	1.0 h at 1050°C / AC	2.5 h at 780°C / AC
F82H	0.5 h at 1040°C / AC	1.5 h at 740°C / AC

The disks were irradiated in HFIR in the capsules of HFIR-MFE-JP-17 and JP-18 at nominal irradiation temperatures of either 90°C or 250°C to neutron fluences producing ~3 dpa. The helium concentration was about 2 and 30 appm in F82H and HT9, respectively.

TEM specimens were thinned using an automatic Tenupol electropolishing unit located in a hot cell. TEM disks were examined using a JEM-2000FX (LaB₆) transmission electron microscope equipped with a special objective lens polepiece that lowers the magnetic field at the ferromagnetic specimen. The foil thicknesses were measured by thickness fringes in order to evaluate quantitative defect density values.

3. Results

3.1 Microstructure of tempered HT9 and F82H

Figure 1 shows the microstructure of tempered HT9 and F82H. In both of them, dislocations were observed with a density of about $1 \times 10^{14} \text{ m}^{-2}$. The tempered F82H contained $M_{23}C_6$ and a few MC carbide, while tempered HT9 contained only $M_{23}C_6$ carbides. The summary of the microstructure, dislocation and precipitates, in HT9 and F82H are given in Table 3. The tempered HT9 contains $M_{23}C_6$ carbides with a number density of $7.0 \times 10^{18} \text{ m}^{-3}$ and mean diameter of 310 nm. In F82H, the number density and mean diameter of $M_{23}C_6$ carbides are higher and smaller than that of tempered HT9, as shown in table 3.

Table 3. The summary of microstructure in HT9 and F82H before irradiation.

Steel	Dislocation	Precipitates		
	Density (m^{-2})	ppt.	Mean diameter (nm)	Number density (m^{-3})
HT9	1×10^{14}	$M_{23}C_6$	310	7.0×10^{18}
F82H	1×10^{14}	$M_{23}C_6$	73	6.0×10^{19}
		MC	14	$< 1 \times 10^{20}$

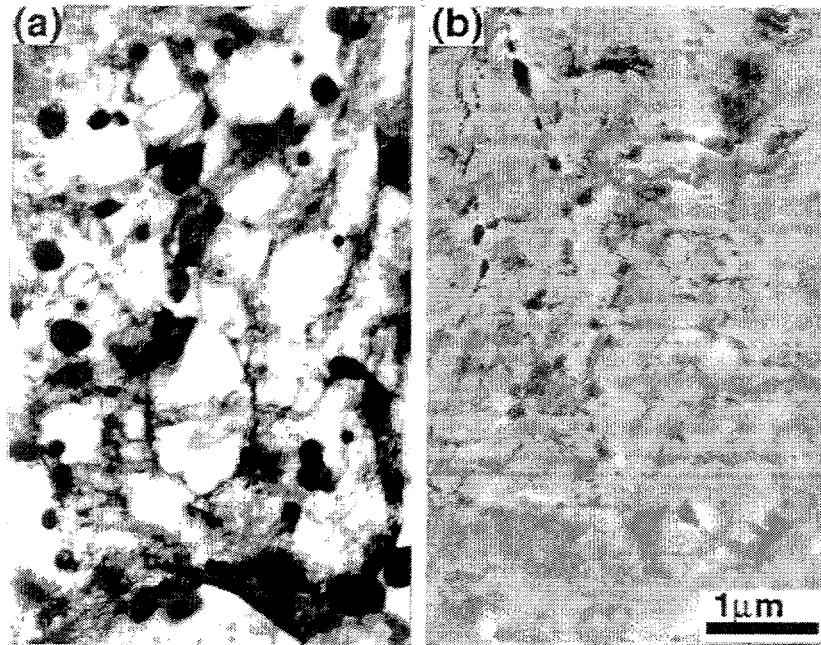


Fig. 1 Microstructures of HT9 (a) and F82H (b) before irradiation.

3.2. Microstructural evolution of HT9 irradiated to ~3 dpa

Figure 2 shows the dislocation segments and loops, which were obtained in HT9 after irradiation at 90°C and 250°C to 3 dpa using the diffraction conditions: $\mathbf{B}=[001]$, $\mathbf{g}=(011)$, (\mathbf{g} , 5 \mathbf{g}). For HT9, the irradiation induced dislocation loop densities of $2.5 \times 10^{21} \text{ m}^{-3}$ and $1.7 \times 10^{22} \text{ m}^{-3}$ with mean diameters of 5 nm and 5 nm, respectively. The dislocation loops in the specimen irradiated at 90°C were perfect types of $\mathbf{b} = a_0 \langle 100 \rangle$ on $\{100\}$, while irradiation at 250°C induced loops of perfect types of not only $\mathbf{b} = a_0 \langle 100 \rangle$ on $\{100\}$ but also $\mathbf{b} = (a_0/2) \langle 111 \rangle$ on $\{111\}$. The total dislocation density, which means the total line length of the dislocation loops, irradiated at 250°C is larger than that at 90°C. Table 4 summarizes the quantitative results for dislocation loops and total dislocation density.

Table 4. The dislocation density of HT9 before and after irradiation at 90°C and 250°C to 3 dpa.

Condition	Dislocation loop		Total
	Number density (m^{-3})	Mean diameter (nm)	Dislocation density (m^{-2})
Before irradiation	-	-	$< 1 \times 10^{14}$
Irr. at 90°C	2.5×10^{21}	5	4.0×10^{13}
Irr. at 250°C	1.7×10^{22}	5	2.6×10^{14}

HT9 contained M_{23}C_6 carbide before irradiation, the irradiation at 90°C caused minor changes in these precipitates, but induced no other carbides. In the HT9 irradiated at 250°C, a radiation-induced phase, tentatively identified as α' , was observed with a number density of $1 \times 10^{20} \text{ m}^{-3}$. Fig. 3 shows a micrograph of α' precipitates, which was taken by using the 2.5 dimension method on weak beam dark-field conditions: $\mathbf{B}=[133]$, $\mathbf{g}=(110)$, (\mathbf{g} , 5 \mathbf{g}). The summary of precipitates before and after irradiation at 90°C and 250°C to 3 dpa is given in Table 5.

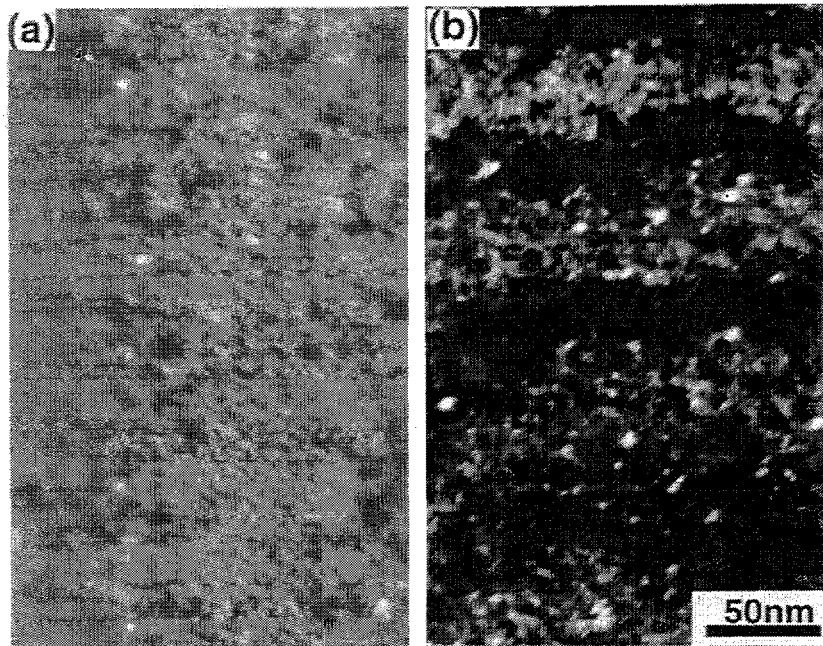


Fig. 2 Microstructures of the dislocation segments and loops in HT9 after irradiation at 90°C (a) and 250°C (b), the diffraction conditions: $B=[001]$, $g=(011)$, (g , $5g$).

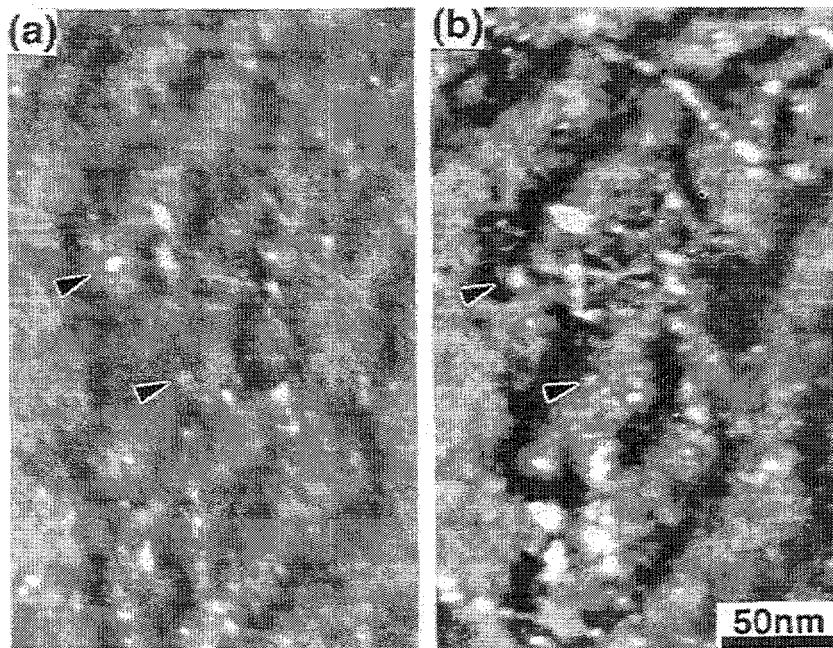


Fig. 3 A stereo-pair of α' precipitates in HT9 irradiated at 250°C to 3 dpa. (a) and (b) are taken with overfocus and underfocus conditions, respectively, on weak beam dark-field conditions: $B=[133]$, $g=(110)$, (g , $5g$).

Table 5. Precipitate statistics in HT9 before and after irradiation at 90°C and 250°C to 3 dpa.

Steel	ppt.	Before irradiation		After irradiation (90°C)		After irradiation (250°C)	
		Mean diameter (nm)	Number density (m ⁻³)	Mean diameter (nm)	Number density (m ⁻³)	Mean diameter (nm)	Number density (m ⁻³)
HT9	M ₂₃ C ₆	310	7.0x10 ¹⁸	310	6.8x10 ¹⁸	313	6.4x10 ¹⁸
	α'	-	-	-	-	<4	<1x10 ²⁰

3.3. Microstructure of F82H irradiated to ~3 dpa

Figure 4 shows the dislocation segments and loops, which formed on {111} planes with $(a/2)\langle 111 \rangle$ Burgers vectors, in F82H after irradiation at 250°C to 3 dpa. The irradiation at 250°C induced a higher dislocation loop density of $2 \times 10^{22} \text{ m}^{-3}$ with a larger mean diameter of 8 nm in F82H than that in HT-9 ($5 \times 10^{21} \text{ m}^{-3}$ with 5 nm). Table 6 summarizes the quantitative results of dislocation loops and total dislocation density.

Table 6. The dislocation density of F82H before and after irradiation at 250°C.

Condition	Dislocation loop		Total
	Number density (m ⁻³)	Mean diameter (nm)	Dislocation density (m ⁻²)
Before irradiation			1x10 ¹⁴
Irr. at 250°C	2x10 ²²	8	5x10 ¹⁴

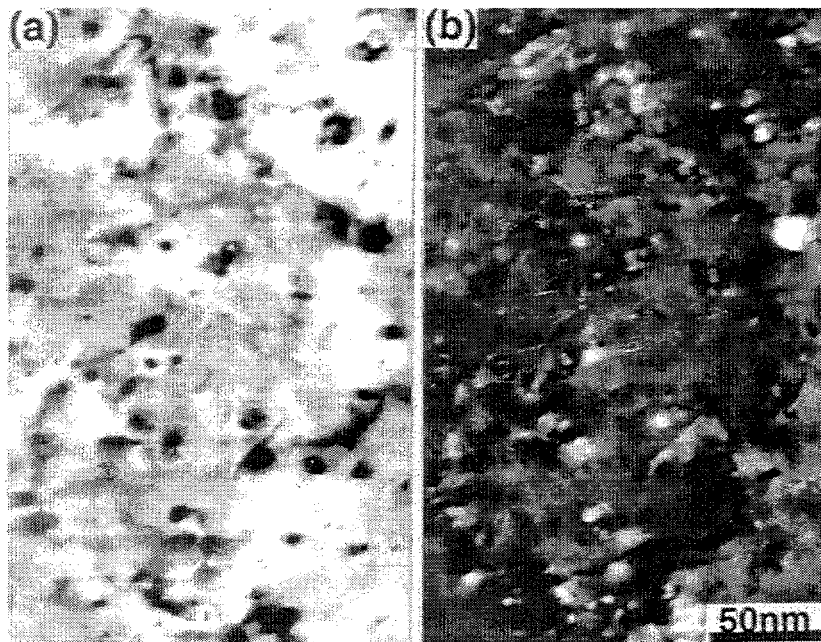


Fig. 4 Micrographs of the dislocation segments and loops in F82H after irradiation at 250°C to 3 dpa. (a) is a bright-field image and (b) is a dark-field image on weak beam dark-field conditions: $\mathbf{B}=[133]$, $\mathbf{g}=(110)$, $(\mathbf{g}, 3\mathbf{g})$.

Before irradiation, the tempered F82H contained $M_{23}C_6$ and a few MC carbides. The irradiation at 250°C to 3 dpa caused minor changes in these precipitates. Table 7 shows summary of precipitates in F82H before and after irradiation at 250°C to 3 dpa. Irradiation at 250°C to 3 dpa caused only minor changes in these precipitates.

Table 7. Precipitate statistics in F82H before and after irradiation at 250°C up to 3 dpa.

Before irradiation			After irradiation (250°C, 3 dpa)		
ppt.	Mean diameter (nm)	Number density (m^{-3})	ppt.	Mean diameter (nm)	Number density (m^{-3})
$M_{23}C_6$	73	6.0×10^{19}	$M_{23}C_6$	73	5.8×10^{19}
MC	14	$< 1 \times 10^{20}$	MC	13	1×10^{20}

4. Discussion

It is well known that ferritic steels have excellent swelling resistance among the alloys considered for fusion structural applications. In this study, the neutron irradiation induced no cavities in both the HT9 and the F82H because of the low irradiation temperatures and low dose.

Before irradiation, there was a significant difference in the distribution of precipitates between the HT9 and the F82H. The HT9 contained a larger amount of $M_{23}C_6$ carbides than the F82H, which is attributed to the HT9 having twice as much carbon. There were no MC carbides in the HT9. The irradiation caused little change in the $M_{23}C_6$ and the MC carbides in both alloys, while, in the HT9 irradiated at 250°C, a low density of precipitates, tentatively identified α' , formed in the matrix. These small particles were detected by using the 2.5 dimension method on weak beam dark-field conditions. It is generally believed that in high-chromium ferritic steels, there is a possibility to form aging embrittlement due to the formation of α' -phase through either spinodal decomposition or nucleation and growth, depending on the aging temperature [3]. Under irradiation, however, the critical content of chromium necessary to form α' -phase may be lower than that during thermal aging. Previous studies of irradiated 12Cr steel [4-6] also reported the particles and identified them as chromium-enriched α' -phase. Mechanical property studies indicate that the HT9 showed a large shift in ductile-brittle transition temperature (DBTT) and a reduction of fracture toughness after irradiation to 3 dpa at 250°C. On the other hand, in the F82H irradiated at 250°C to 3 dpa, the shift of DBTT and the decrease in fracture toughness were less than that in HT9. As discussed in a previous paper [7], it is believed that this phase formed in HT9 may contribute to the decrease in toughness.

The irradiation of HT9 at 90°C and 250°C induced dislocation loops which were perfect types of $b = a_0 \langle 100 \rangle$ on $\{100\}$ and/or $b = (a_0/2) \langle 111 \rangle$ on $\{111\}$. Total dislocation density irradiated at 250°C is larger than that at 90°C because of the higher number density. On the other hand, irradiation of F82H at 250°C induced dislocation loops on $\{111\}$ planes with $(a_0/2) \langle 111 \rangle$ Burgers vectors. In Fe-Cr binary alloys, with respect to dislocation evolution in an initially almost dislocation-free condition, interstitial type dislocation loops with an $a_0 \langle 100 \rangle$ and/or $(a_0/2) \langle 111 \rangle$ Burgers vector develop during irradiation [8,9]. According to an investigation of dislocation loop evolution in ferritic alloys irradiated to high fluence [10,11], the $a_0 \langle 100 \rangle$ type dislocation loops were sensitive to chromium content and a number of $a_0 \langle 100 \rangle$ type dislocation loops were present in Fe-12Cr alloy irradiated at 420°C to 140 dpa, while in the Fe-6Cr and Fe-9Cr alloys, their number density was extremely low. This difference of the nucleation of interstitial loops could be explained by chromium stabilization of interstitial clusters, and/or α' precipitation promotes the loop nucleation in Fe-12Cr alloy. On the other hand, according to previous paper which

investigated a relationship between type of dislocation loop and content of interstitial impurities, there is a tendency for $a_0\langle 100 \rangle$ type loop to form in low-purity alloys [12]. The HT9 used in this study has twice as much carbon and ten times as much nitrogen as the F82H, and there is a possibility that the difference in impurity content affects loop formation. The growth rate of loops should be controlled by not only dislocation bias for interstitials and vacancies but also the stability, i.e., the strain energy, of loops [12], the differences of the growth rate and the number density between $a_0\langle 100 \rangle$ and $(a_0/2)\langle 111 \rangle$ type loops at lower temperature should be investigated. It is possible that these differences in evolution of dislocation loops and radiation-induced phases during irradiation could be related to the different post-yield deformation behavior observed in the two alloys.

FUTURE WORK

Further analysis will be carried out of the relationships between the microstructural parameters and the measured flow and fracture properties.

ACKNOWLEDGMENTS

The authors are grateful to Dr. M.L. Grossbeck for providing valuable irradiated samples. They also would like to thank Drs. R.L. Klueh and S.J. Zinkle for their helpful discussions. This research was supported in part by an appointment to the Oak Ridge National Laboratory Postdoctoral Research Associates Program administered jointly by the Oak Ridge Institute for Science and Education and Oak Ridge National Laboratory, and sponsored by the Office of Fusion Energy Sciences, U.S. Department of Energy, under contact DE-AC05-96 OR22464 with Lockheed Martin Energy Research Corp., and the Japan Atomic Energy Research Institute.

REFERENCES

- 1) R.L. Klueh, K. Ehrlich, and F. Abe, *J. Nucl. Mater.* **191-194** (1992) 116.
- 2) D.J. Alexander, J.E. Powell, M.L. Grossbeck, A.F. Rowcliffe, and K. Shiba, *Effects of Radiation on Materials: 17th International Symposium*, ASTM STP 1270, D.S. Gelles, R.K. Nanstad, A.S. Kumar, and E.A. Little, Eds., American Society for Testing and Materials, Philadelphia, PA (1996) p. 945
- 3) *Metals Handbooks*, 10th Ed., Vol. 1 (American Society for Metals, Metals Park, PA, 1992)
- 4) J.J. Kai and R.D. Lee, *J. Nucl. Mater.* **175** (1990) 227.
- 5) P. Dubuisson, D. Gibson, and J.L. Seran, *J. Nucl. Mater.* **205** (1993) 178.
- 6) D.S. Gelles, *Effects of Radiation on Materials: 14th International Symposium*, ASTM STP 1046, N.H. Packan, R.E. Stoller, and A.S. Kumar, Eds., American Society for Testing and Materials, Philadelphia, PA (1990) p. 73.
- 7) R.L. Klueh, J.J. Kai, and D.J. Alexander, *J. Nucl. Mater.* **225** (1995) 175.
- 8) N. Yoshida, et al., *J. Nucl. Mater.*, **155-157** (1988), 1232.
- 9) D.S. Gelles, Annual Progress Report for Fusion Year, (1991), 348.
- 10) Y. Katoh, A. Kohyama and D.S. Gelles, *J. Nucl. Mater.*, **225** (1996) 154.
- 11) D.S. Gelles, *J. Nucl. Mater.*, **225** (1995) 163.
- 12) E. Wakai et al., *Proceeding of Ultra High Purity Base metals*, UHPM-94, 488.